Astron. Astrophys. 308, 465–471 (1996)

ASTRONOMY AND ASTROPHYSICS

Radiation-driven envelopes around magnetic white dwarfs

Radiation-driven diskons

Vladimir V. Zheleznyakov[1], **A.V. Serber**[1], **and Jan Kuijpers**[2,3,4]

[1] Institute of Applied Physics, Russian Academy of Science, Nizhny Novgorod, Russia
[2] Sterrekundig Instituut Utrecht, Postbus 80.000, 3508 TA Utrecht, The Netherlands
[3] Centrum voor Hoge- Energie Astrofysica, P.O. Box 41882, 1009 DB Amsterdam, The Netherlands
[4] Dep. High Energy Physics, University of Nijmegen, Toernooiveld 1, 6525 ED Nijmegen, The Netherlands

Received 1 December 1994 / Accepted 30 June 1995

Abstract. We investigate the formation of a plasma envelope in the magnetosphere of a hot white dwarf by cyclotron radiation pressure. The radiation pressure distribution (both in the continuum and in the cyclotron line) is derived for an optically thin, dipolar magnetosphere of an isolated, non-rotating star emitting blackbody radiation. For an isothermal, fully ionized, pure hydrogen plasma the hydrostatic solution consists of a closed plasma shell accumulated in a potential well near the equilibrium surface, where radiation pressure cancels gravity, and an equatorial disk inside this surface. The presence of a finite optical depth leads to a temporal variation of the plasma envelope and of the observed radiation. We apply these results to the strongly magnetized white dwarf GD 229, which is a candidate for such a radiation-driven envelope or "diskon". The deep unidentified 2000-3000 Å depression in its UV spectrum is explained as the result of cyclotron scattering in optically thick gyroresonant layers around the star. We predict a temporal and spectral variability of this feature with a characteristic time of $\geq$ 1 hr due to non-stationary plasma motions in the envelope.

Key words: chaos – stars: individual: GD 229 – stars: magnetic fields – stars: white dwarfs – ultraviolet: stars

1. Introduction

Since the early eighties (Mitrofanov and Pavlov 1982) it is known that cyclotron radiation pressure can significantly affect the force balance of plasma near magnetized white dwarfs and neutron stars. In particular, cyclotron pressure can decelerate matter in the accretion column above an X-ray pulsar (e.g. see Braun and Yahel, 1984; Zheleznyakov and Litvinchuk, 1986; Herold et al., 1987; Arons, 1987), reduce the critical luminosity of a magnetized degenerate star and drive a wind from its surface (Mitrofanov 1986; Zheleznyakov and Litvinchuk 1987; Zheleznyakov and Serber 1991, 1994), or form peculiar plasma structures in the magnetospheres of such stars (Bespalov and Zhelez nyakov 1990; Bespalov et al. 1990; Dermer and Sturner 1991; Sturner and Dermer 1992, 1994). In the model by Bespalov and Zheleznyakov (1990) a hot, magnetized, degenerate star sustains a wind driven from the photosphere by cyclotron radiation pressure, a dense plasma disk at the magnetic equator, and two jets along the polar field lines. Such an object as a whole has been called *radiation- driven diskon*. This model has been based on the simplifying assumption of an inverse square law for the radial dependence of the radiation pressure force which is valid for a flat spectrum or a constant magnetic field. The more realistic case of a dipolar field exposed to blackbody radiation from the photosphere has been considered by Dermer and Sturner (1991), Sturner and Dermer (1992). They found that the component of the cyclotron radiation pressure force along a field line has a maximum at the locations where the local gyrofrequency equals the frequency of the peak of the blackbody spectrum. As a result, there may exist one or two equilibrium regions where the radiation pressure force cancels the force of gravity. The outer region is stable while the inner one (if any) is unstable. In their further application to (accreting) X-ray pulsars Sturner and Dermer (1994) showed that the radiation from a polar hot spot is able to support a lampshade-like envelope around the accretion funnel which leads to temporally varying pulse profiles. In the present paper we restrict ourselves to white dwarfs which at present constitute the best candidates for winds driven by cyclotron radiation pressure (Zheleznyakov and Serber 1991, 1994) and analyze the structure and temporal behavior of the envelope in more detail. A similar analysis for neutron stars will be given elsewhere.

2. Radiation pressure in an optically thin magnetosphere

Whereas Dermer and Sturner (1991) calculated the radiation force by scattering on a stationary electron at the ground

Send offprint requests to: V.V. Zheleznyakov

Landau level in vacuum, we derive the radiation force density, $\boldsymbol{f}_{\rm rad}$, in an optically thin plasma with a Maxwell distribution over the longitudinal momenta. At a given point in the magnetosphere the force $\boldsymbol{f}_{\rm rad}$ depends on the intensity of the photospheric radiation reaching this point and comprises both a term due to magnetic Thomson scattering in the continuum, $\boldsymbol{f}_c$, and a term due to extinction of radiation in the cyclotron line, $\boldsymbol{f}_B$ (see, for example, Zheleznyakov and Serber 1991, 1994). Both true absorption and scattering events contribute to the latter component and their relative importance is given by $\epsilon \simeq 4 \cdot 10^{-7}(B/10^8\,{\rm G})^{-2}(T_\parallel/10^7\,{\rm K})^{-3/2}$ $(N/10^{10}\,{\rm cm}^{-3})$, which is the ratio of the spontaneous cyclotron transition time, $(3mc^3/4e^2\omega_B^2)$, to the time between collisions (Zheleznyakov 1984, Zheleznyakov and Litvinchuk 1984). Further we will assume that the inequality $(1/45\pi)(e^2/\hbar c)(B/B_c)^2 \ll \omega_p^2/(\beta_{T_\parallel}\omega_B^2)$ is satisfied, where ω_p is the electron plasma frequency, ω_B is the electron gyrofrequency, $\beta_{T_\parallel} = \sqrt{\kappa T_\parallel/mc^2}$, $B_c = m^2c^3/\hbar e \simeq 4.14 \cdot 10^{13}$ G, $T_\parallel$ is the electron temperature along the magnetic field direction and N is the electron density of the magnetospheric plasma. In this case the polarization of the electromagnetic modes is determined by the rarefied plasma and not by vacuum birefringence in a strong magnetic field (Zheleznyakov 1984). Both modes are elliptically polarized, the ellipse of polarization being similar to the projection of the electron Larmor circle onto the plane perpendicular to the wave vector. The electric field vector of the extraordinary mode ($l = 1$) rotates in the same direction as an electron in the magnetic field, while the opposite is true for the ordinary mode ($l = 2$). These polarizations are different from the linear polarizations of the vacuum modes used by Dermer and Sturner (1991)) and are responsible for the weak interaction of the ordinary radiation with the rarefied plasma. The ratio of the corresponding opacities at the first harmonic is $\chi_{12}/\chi_{11} \sim \beta_{T_\parallel}^2 \ll 1$, so that we can neglect the contribution of the ordinary mode to the cyclotron line radiation force $\boldsymbol{f}_B$ in an optically thin plasma. Radiative transfer in the photospheres of magnetized degenerate stars is discussed in detail by Zheleznyakov (1981), Zheleznyakov and Serber (1991, 1994) and we shall use their results. Every point of the photosphere emits a blackbody spectrum with a deep and sharp "Fraunhofer" cyclotron line in absorption in the extraordinary component at the local photospheric gyrofrequency, ω_{B_*}. The residual intensity in the center of this line with respect to the continuum is characterized by the parameter $M_{B_*} = \epsilon/\tau_c$ and is about equal to $M_{B_*}^{1/3} \simeq 8.85 \cdot 10^{-2}\,(g/10^8\,{\rm cm/s^2})^{1/3}\,(B_*/10^8\,{\rm G})^{-1/3}\,(T_*/10^4\,{\rm K})^{-2/3}$ and its width is $\simeq 3\sqrt{2}\beta_{T_*}\omega_{B_*}$. Here τ_c is the optical depth in the center of the cyclotron line from the top of the photosphere downwards. Due to its narrowness the effect of the line on $\boldsymbol{f}_c$ is small, while its effect on $\boldsymbol{f}_B$ can be neglected if the line does not overlap with the cyclotron resonance peak (which is downshifted with respect to ω_{B_*}) in the opacity of the magnetospheric plasma. For a magnetic dipole the magnetospheric cyclotron resonance peak has a width of $3\sqrt{2}\beta_{T_\parallel}\omega_B$ and is centered at $\omega_B = (\omega_{B_p}/2\rho^3)\sqrt{1+3\cos^2\Theta}$, where ω_{B_p} corresponds to the polar field strength B_p, Θ is the angle between the magnetic axis and the radius vector $\boldsymbol{r}$ from the stellar center, $\rho = r/R_*$, and R_* is the stellar radius. Overlap only exists in the small part of the magnetosphere given by

$$1 \le \rho \le \rho_{\rm line}(\Theta)\left[1 + \frac{3\sqrt{2}(\beta_{T_\parallel} + \beta_{T_*})}{2 + \rho_{\rm line}^6(\Theta)\frac{1+3\sin\Theta(\sin\Theta - |\cos\Theta|)}{1+3\cos^2\Theta}}\right], \quad (1)$$

where $\max\{\rho_{\rm line}(\Theta)\} \approx 1.115$ in directions close to $\Theta = \pi/4, 3\pi/4$. The function $\rho_{\rm line}(\Theta)$ is determined in the appendix and is shown with the thin line in Fig. 2 just outside the star. Radiation pressure in region (1) will be considered elsewhere. As for the rest of the magnetosphere, the intensity of the diluted photospheric continuum can be used for calculating the radiation pressure:

$$I_{\omega l}(\rho,\Theta,\omega,\vartheta,\phi) = B^*(\omega){\rm H}(\cos\vartheta - \sqrt{1-\rho^{-2}}). \quad (2)$$

Here

$${\rm H}(x) = \begin{cases} 1 & \text{if } x \ge 0 \\ 0 & \text{otherwise} \end{cases} \quad (3)$$

is the step function;

$$B^*(\omega) = \frac{\hbar\omega^3}{8\pi^3c^2}\,(\exp(\frac{\hbar\omega}{\kappa T_*}) - 1)^{-1} \quad (4)$$

is the blackbody intensity at a photospheric temperature T_* in one mode; ϑ is the angle between $\boldsymbol{n}$, the unit vector along a ray, and $\boldsymbol{r}$; ϕ is the angle between $\boldsymbol{n}$ and $\boldsymbol{r}$-$\boldsymbol{B}$ plane. With this choice

$$\boldsymbol{f}_c \simeq \frac{\sigma_{Th}}{2c}\int_0^\infty d\omega \int_0^{2\pi} d\phi \int_{-1}^1 d\cos\vartheta$$

$$\sum_{l=1,2}\left[1 + \frac{\omega^2}{(\omega + (-1)^l\omega_B)^2}\right]\boldsymbol{n}\,I_{\omega l} \simeq$$

$$\frac{\sigma_{Th}}{c}\left(\sigma T^4 + \pi B^*(\omega_B)\frac{\omega_B}{3\sqrt{2}\beta_{T_\parallel}}\right)\frac{\hat{\boldsymbol{r}}}{\rho^2} \quad (5)$$

and

$$\boldsymbol{f}_B \simeq \frac{2\pi^2e^2}{mc^2}\int_0^{2\pi} d\phi \int_{-1}^1 d\cos\vartheta(1+\cos^2\alpha)\,\boldsymbol{n}\,I_{\omega 1}(\omega_B)$$

$$= \left[\hat{\boldsymbol{r}}\left(1 + \cos^2\delta + \frac{1-3\cos^2\delta}{4\rho^2}\right) + \hat{\boldsymbol{\Theta}}\,\frac{\sin\delta\cos\delta}{2\rho^2}\right] f_B, \quad (6)$$

where

$$f_B = \frac{2\pi^3e^2}{mc^2}\frac{B^*(\omega_B)}{\rho^2} = \frac{m_p g}{\rho^2}\Gamma, \quad (7)$$

$$\Gamma \simeq 1.2\left(\frac{T_*}{10^4\,{\rm K}}\right)^3\left(\frac{g}{10^8\,{\rm cm/s^2}}\right)^{-1}\frac{b^3}{e^b - 1}, \quad (8)$$

σ is the Stefan-Boltzmann constant, σ_{Th} is the Thomson cross section, m_p the proton mass, g the gravitational acceleration at the stellar surface, $\alpha = \arccos(\cos\vartheta\cos\delta +$

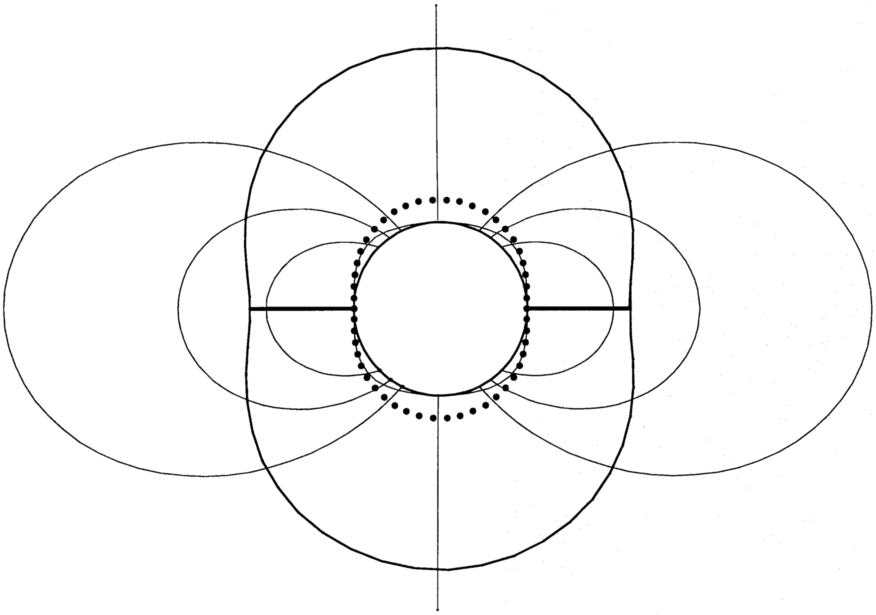

Fig. 1. Radiation-driven envelope of the magnetic white dwarf GD 229. The star and the equilibrium surface are shown with thick lines, the dipole field lines are indicated by thin lines, and a thin line just above the stellar photosphere denotes the border $\rho_{\rm line}(\Theta)$ (see (1)). Optically thin plasma accumulates near the equilibrium surface and also on the equatorial plane between this surface and the star. Eventually an optically thick envelope extends from the star to the equilibrium surface. Cyclotron scattering in this envelope gives rise to a strong feature in the spectrum of the star. The filled circles mark the gyroresonant layer which correspond to the blue edge ($\approx$ 2000 Å) of the unidentified depression in the spectrum of GD 229.

$\sin\vartheta\sin$ delta $\cos\phi$) is the angle between $\boldsymbol{n}$ and $\boldsymbol{B}$, $b = \hbar\omega_B/\kappa T_* = 1.28(B/10^8\,{\rm G})(T_*/10^4\,{\rm K})^{-1}$, and $\delta = \arccos(2\cos\Theta(1+3\cos^2\Theta)^{-1/2})$ is the angle between $\boldsymbol{r}$ and $\boldsymbol{B}$. Note that $|\boldsymbol{f}_c| \ll |\boldsymbol{f}_B|$ for $B \simeq 10^8 - 10^{10}$ G and $T_* \ll T_{\rm cr}$ (where $T_{\rm cr} = 6.2\cdot 10^5 (g/10^8\,{\rm cm/s^2})^{1/4}$ K is the critical, or Eddington, temperature). Below we will therefore only take into account $\boldsymbol{f}_B$. The longitudinal and transverse components of this force with respect to the dipole magnetic field are given by

$$f_B^{\|;\perp} = f_B\left[1+\cos^2\delta+\frac{\{3;1\}-5\cos^2\delta}{4\rho^2}\right]\{\cos\delta;\sin\delta\}. \quad (9)$$

2.1. Magnetohydrostatic radiation-supported envelope

Consider now the effect of the cyclotron force (6) on the magnetospheric plasma. Here we restrict ourselves to the analysis of a static configuration in closed magnetic shells when the motion of plasma across the strong field is suppressed. The pressure distribution of a fully ionized, pure hydrogen plasma along the field lines can be found from the equation

$$\frac{dp}{dl} = N f_B^{\|} - N m_p g \rho^{-2}\cos\delta, \quad (10)$$

in which p=$2N\kappa T$. If, moreover, the plasma is isothermal, the equation for the density N follows from (10):

$$\rho^2 \frac{H}{R_*}\frac{d\ln N}{d\rho} = \left[1+\cos^2\delta+\frac{3-5\cos^2\delta}{4\rho^2}\right]\Gamma - 1 \quad (11)$$

where $H = 2\kappa T_{\|}/m_p g$. Note that $\Gamma \gg 1$ near the surface of a white dwarf with radiation driven ejection of plasma from the photosphere, but that it drops rapidly with distance due to the decreasing magnetic field strength and the resulting shift of ω_B into the Rayleigh-Jeans part of the photospheric spectrum where $\Gamma \propto \omega_B^2$. As a result, for any Θ there is a value for ρ=$\rho_0(\Theta)$ at which the longitudinal components of the radiation pressure force and the force of gravity are exactly balanced. These points form a surface of stable equilibrium for the magnetospheric plasma. This equilibrium surface is analogous to the outer one in Dermer and Sturner (1991), Sturner and Dermer (1992). The inner, unstable, equilibrium surface in these papers can only appear in the magnetosphere if the radiation force near the stellar surface is less than the force of gravity. For the stars considered here the inner equilibrium surface is located inside the photosphere and has been analyzed by Zheleznyakov and Serber (1991, 1994). The shape of the equilibrium surface can be determined by putting to zero the right-hand side of (11). An example of such a surface $\rho_0(\Theta)$ is shown in Fig. 2 with thick lines. It crosses the polar field line at a distance $\rho_0^{\rm pol}$ which is determined by

$$(\rho_0^{\rm pol})^9[\exp(b_p(\rho_0^{\rm pol})^{-3}) - 1] = 2\Gamma_p^{\rm RJ} b_p(1 - 1/(2\rho_0^{\rm pol})^2), \quad (12)$$

where $\Gamma_p^{\rm RJ} \simeq 2(B_p/10^8\,{\rm G})^2(T_*/10^4\,{\rm K})(g/10^8\,{\rm cm/s^2})^{-1}$ and b_p=$\hbar\omega_{B_p}/\kappa T_*$. The surface crosses the magnetic equator at a distance $\rho_0^{\rm eq}$ determined by

$$(\rho_0^{\rm eq})^9[\exp(b_p/2(\rho_0^{\rm eq})^3) - 1] = \Gamma_p^{\rm RJ} b_p(1+3/(2\rho_0^{\rm eq})^2)/8. \quad (13)$$

Note that $\rho_0^{\rm pol} > \rho_0^{\rm eq}$. Note also that the part of the magnetic equator where $1 \le \rho \le \rho_0^{\rm eq}$ also forms an equilibrium surface for magnetospheric plasma, since the radiation pressure force exceeds gravity all along the field lines crossing this region, so that a net force is directed towards the equatorial plane, while on this plane the longitudinal components of $\boldsymbol{f}_B$ and $m_p g \boldsymbol{r} R_*^2/r^3$ vanish (see also Bespalov and Zheleznyakov 1990). To determine the plasma distribution near the equilibrium surface we expand the right-hand side of (11) in $\tilde\rho$=$\rho - \rho_0 \ll \rho_0$ and find that

$$N(\tilde\rho) = N_0\exp\left(\frac{\tilde\rho^2}{\Delta^2}\right), \quad (14)$$

where N_0 is the plasma density at the equilibrium surface,

$$\Delta = \rho_0^{3/2}\sqrt{\frac{H}{R_*}\mathsf{D}}$$

$$\simeq 0.04\rho_0\left(\frac{T/10^6\mathrm{K}}{(g/10^8\mathrm{cm/s^2})(R_*/10^9\mathrm{cm})}\rho_0\mathsf{D}\right)^{1/2} \ll \rho_0 \quad (15)$$

is the characteristic scale length of the plasma density,

$$\mathsf{D}^{-1} = 3 + \frac{3}{2}\left(1 - \frac{b_0}{1-\mathrm{e}^{-b_0}}\right)\left(1+\frac{\sin^2\delta}{2}\right)$$

$$+\frac{1}{2}\frac{7\sin^2\Theta - \frac{1}{4\rho_0^2}(5+11\cos^2\Theta)}{1+7\cos^2\Theta + \frac{1}{4\rho_0^2}(3-11\cos^2\Theta)}, \quad (16)$$

and $b_0 = b_p\sqrt{1+3\cos^2\Theta}/2\rho_0^3$. The total number of particles in the potential well near the equilibrium surface can be estimated as follows:

$$N_0^{\mathrm{tot}} = 2\pi R_*^3 \int_0^{\pi}\int_{-\infty}^{\infty} N(\tilde\rho)d\tilde\rho\ \rho_0^2(\Theta)\sin\Theta d\Theta$$

$$\approx 4\pi^{3/2}R_*^3\rho_0^2 N_0\Delta. \quad (17)$$

The above hydrostatic model applies also to a slowly accumulating plasma layer near the equilibrium surface if the magnetospheric plasma remains optically thin and if the dynamical pressure of the photospheric wind is negligible compared to the plasma pressure in the magnetosphere. In the absence of a proper theory for the photospheric wind we will assume the latter condition to be fulfilled. The former condition can be checked from the value of N_0 which we will estimate in the next section using an upper limit to the mass loss rate from the photosphere.

2.2. Upper limit to the mass loss rate of a magnetic white dwarf

An upper limit to the particle flux J per unit stellar surface area can be obtained from the maximum amount of momentum available in the form of radiation to drive a wind along the field lines (cf. Lucy and Solomon, 1970). Such a wind driven by radiation pressure in the cyclotron line from the photosphere up to a terminal velocity v_{term}, can only get longitudinal momentum of radiation in the frequency interval $(v_{\mathrm{term}}/c)\omega_{B_*}$ Doppler shifted upwards from the photospheric cyclotron frequeny ω_{B_*}. Therefore the momentum flux of the ejected plasma, $\mathsf{P}_{\mathrm{pl}}=Jm_p v_{\mathrm{term}}$, can not exceed the longitudinal momentum flux of radiation, $\mathsf{P}^{\|}_{\mathrm{rad}}=(\pi B^*(\omega_{B_*})/c)(\omega_{B_*}v_{\mathrm{term}}/c)\cos\delta_*$, so that

$$J_{\max}(\Theta_*) = \frac{\pi B^*(\omega_{B_*})\omega_{B_*}}{m_p c^2}\cos\delta_*$$

$$\simeq 2.8\cdot 10^{13}\left(\frac{T_*}{10^4\,\mathrm{K}}\right)^4 \frac{b_*^4\cos\delta_*}{\mathrm{e}^{b_*}-1}\ \mathrm{cm^{-2}s^{-1}}, \quad (18)$$

where $b_*=\hbar\omega_{B_*}/\kappa T_*$. Averaging J over the stellar surface yields the mass loss rate:

$$\dot M_{\max} = 4\pi R_*^2\int_0^1 m_p J_{\max}\cos\delta_*\, d\cos\Theta_*$$

$$\simeq 2.15\cdot 10^9\left(\frac{R_*}{10^9\mathrm{cm}}\right)^2\left(\frac{B_p}{10^8\mathrm{G}}\right)^4$$

$$\int_{1/2}^1 \frac{x^3}{\mathrm{e}^{xb_p}-1}\sqrt{\frac{4x^2-1}{3}}dx \mathrm{g/s}, \quad (19)$$

where $b_p=\hbar\omega_{B_p}/\kappa T_*$. If a wind already exists at the level of the photosphere a similar reasoning applies now however replacing ω_{B_*} with the maximum cyclotron frequency occurring inside the star.

2.3. The effect of a finite optical depth

With the above estimate of $\dot M$ it is possible to determine the minimum time needed to accumulate an optically thick envelope. Plasma in the nonuniform magnetic field around a white dwarf interacts with radiation mainly via cyclotron scattering in so-called gyroresonant layers with a size $l_B \simeq 2\sqrt{2}\,\beta_{T_\|}L_B|\cos\alpha|$ (Zheleznyakov 1984; Zheleznyakov and Litvinchuk 1986) situated near surfaces where the radiation frequency equals the local gyrofrequency, $\omega = \omega_B$ (here $L_B = B|(\boldsymbol{n}\cdot\nabla)B|^{-1}\simeq\rho R_*/3$ is the characteristic scale of the dipole magnetic field). The optical depth of a gyroresonant layer is equal to

$$\tau_g = \frac{2\pi^2 e^2 N L_B}{mc\omega_B}(1+\cos^2\alpha). \quad (20)$$

The gyroresonant layer near the equilibrium becomes therefore optically thick in a time

$$t_0 \ge m_p N_0^{\mathrm{tot}}/\dot M_{\max} \quad (21)$$

where N_0^{tot} is determined by (17) with the density N_0 at the equilibrium surface matching the condition $\tau_g(N_0) = 1$. Taking into account that $B \propto \rho^{-3}$ for the dipole configuration, and approximating $\sqrt{\pi/\mathsf{D}\rho_0}\sim 1$, we finally find:

$$t_0 \ge 8.5\left(\frac{B_p}{10^8\mathrm{K}}\right)^{-3}\left(\frac{T/10^6\mathrm{K}}{(g/10^8\mathrm{cm/s^2})(R_*/10^9\mathrm{cm})}\right)^{0.5}$$

$$\left(\int_{1/2}^1\frac{x^3}{\mathrm{e}^{xb_p}-1}\sqrt{\frac{4x^2-1}{3}}dx\right)^{-1}\ \mathrm{s}. \quad (22)$$

This time is very small for white dwarf conditions. So, a model with optically thick plasma is more adequate to describe the envelope. Leaving the detailed discussion of such a model to a subsequent publication, we briefly describe here the general structure and behavior of an optically thick plasma in the magnetosphere. Firstly, we correct the force (6) for a non-vanishing τ_g (Zheleznyakov and Litvinchuk 1986):

$$f_B^{\|}(\tau_g) \simeq f_B^{\|}\min\{1,\tau_g^{-1}\}. \quad (23)$$

As matter is pumped upwards from the photosphere the optical depth τ_g increases and the radiation force density decreases. The density increase between the equilibrium layer and the stellar surface continues until the inequality $m_p g\rho^{-2}\cos\delta < f_B^{\|}(\tau_g)$

no longer holds. Thereafter the local plasma density remains constant at a level ensuring an "optically thick equilibrium":

$$\tau_g(\rho) \simeq \Gamma. \tag{24}$$

A further increase of N is impossible because the total radiative momentum in the frequency band $\beta_{T_\parallel}\omega_B$ is now intercepted, and the resulting radiation force on the gyroresonant layer can not support more plasma againt gravity. This can be easily seen by rewriting condition (24) in the following form:

$$\frac{\pi B^*(\omega_B)}{c}\beta_{T_\parallel}\omega_B\frac{1}{\rho^2} \simeq \frac{m_p g}{\rho^2} N l_B. \tag{25}$$

As plasma continues to be injected, the region $1 \leq \rho \leq \rho_0$ between the stellar surface and the equilibrium layer becomes filled with plasma of density

$$N_g(\rho,\Theta) \simeq \frac{\pi B^*(\omega_B)\omega_B}{c}\frac{1}{m_p g L_B} \tag{26}$$

set by condition (24). Thereafter the photospheric radiation field is unable to support the dense envelope. This leads to a rapid collapse and downfall of plasma onto the star in about a free-fall time. As a result, the magnetosphere becomes optically thin, and the envelope starts to be built up again. The strong radiation pressure therefore drives non-stationary density pulsations in the region $1 \leq \rho \leq \rho_0$ because of the effect of finite optical thickness. The characteristic time of the pulsations is given by the formation time of the density profile (24) in this region:

$$t_g \simeq m_p N_g^{\rm tot}/\dot{M}_{\rm max} \tag{27}$$

where

$$\frac{N_g^{\rm tot}}{4\pi R_*^2} = \int_0^1 R_* d\cos\Theta \int_1^{\rho_0(\Theta)} N_g(\rho,\Theta)\,,\rho^2 d\rho$$

$$\geq \frac{\sigma T_*^4 b_p^4}{m_p g c}\frac{15}{2\pi^4}\int_0^1 \sqrt[3]{\frac{1+3\cos^2\Theta}{4}}\,d\cos\Theta\int_{\rho_0^{-3}(\Theta)}^1 \frac{x^{4/3}dx}{e^{xb_p}-1}. \tag{28}$$

Taking into account (19), we find the following estimate

$$t_g \geq \frac{175}{g/10^8\,{\rm cm/s^2}}$$

$$\int_{1/(\rho_0^{\rm eq})^3}^1 \frac{x^{4/3}dx}{e^{xb_p}-1}\left(\int_{1/2}^1 \frac{x^3}{e^{xb_p}-1}\sqrt{\frac{4x^2-1}{3}}dx\right)^{-1} {\rm s}. \tag{29}$$

The presence of the radiation-driven envelope has an important effect on the observed radiation from the star. As has been shown by Zheleznyakov and Litvinchuk (1986) a scattering gyroresonant layer with $\tau_g \gg 1$ reflects nearly half of the incoming extraordinary mode radiation, while the intensity of the ordinary component is not changed due to its weak interaction with the rarefied magnetospheric plasma (see section 2). Therefore, when the gyroresonant region $1\leq\rho\leq\rho_0$ is completely optically thick, a depression is present in the observed radiation over a frequency interval $\omega_B(\rho_0(\Theta)) \leq \omega \leq \omega_{B_*}$ with a residual intensity

$$r = \frac{I_{\omega 1}(\omega) + I_{\omega 2}(\omega)}{2B^*(\omega)} \sim 3/4 \tag{30}$$

compared to a blackbody continuum. This spectral feature is expected to vary with the characteristic time (29) of the plasma pulsations in the magnetosphere.

3. Application to the white dwarf GD 229

Cyclotron radiation pressure is expected to play a role in the atmospheres of white dwarfs PG 1031+234, GrW +70°8247 and GD 229 (Zheleznyakov and Serber 1994). The strongly magnetic GD 229 is probably the most peculiar of white dwarfs known. The linear polarization of its optical continuum $P_l \simeq 4$ % (West 1989) requires the presence of a strong magnetic field. The star has an extremely rich spectrum of absorption features in the optical band. Attempts to explain the peculiar stellar spectrum by the effect of a strong magnetic field on a hydrogen spectrum (Forster et al. 1984; Henry and O'Connel 1985) have failed as the entire optical spectrum can not be explained by transitions in magnetized hydrogen for field strengths up to $2\cdot10^9$ G (Schmidt et al. 1990). Therefore it has been suggested that the observed optical features are due to neutral helium (or may be carbon). However this hypothesis can not be tested as calculations of HeI transitions in a magnetic field are not yet extended beyond the present limit of perturbation theory. Fortunately, GD 229 is sufficiently close (29 pc; Dahn et al. 1982) and hot ($T_* \sim (1.6-2)\cdot 10^4$ K; Green and Liebert 1981) to be accessible to *IUE*. The UV deficit in the interval ~2000-3000 Å, pointed out by Green and Liebert (1981), appears as an immense depression when combined with the optical spectrum (Schmidt et al. 1990). After more than a decade since its discovery these puzzling features at UV and optical wavelengths remains unexplained. In our opinion it seems quite improbable that the broad and deep UV depression can be caused by an atomic transition in a strong magnetic field. Rather we propose an alternative interpretation of the remarkable UV depression in the spectrum of GD 229 in terms of a radiation- driven diskon (Zheleznyakov and Serber 1994). Cyclotron scattering at the first harmonic offers the best explanation for the depression. The scattering takes place in optically thick gyroresonant layers situated in between the photosphere and the equilibrium surface and obscures the entire disk of the star. In this case the blue edge of the strong UV depression corresponds to the gyroresonant layer above the star at the magnetic equator. The layer is shown by filled circles in Fig. 2. With this assumption we find $B_p \simeq 10^9$ G. Using $T_* \simeq 2\cdot10^4$ K and $g \simeq 10^8\,{\rm cm/s^2}$ we find that GD 229 can eject up to $\dot{M}_{\rm max} \simeq 2\cdot10^{10}$ g/s $\simeq 0.015\dot{M}_\odot$ from its surface ($\dot{M}_\odot \simeq 2\cdot10^{-14}\,M_\odot$/yr). This flux can create a shell of plasma near the equilibrium surface with $\rho_0^{\rm eq} \simeq 2.22$ and $\rho_0^{\rm pol} \simeq 3.06$, and moreover a disk in the region $1 \leq \rho \leq \rho_0^{\rm eq}$. The shell becomes optically thick to cyclotron scattering in a time $t_0 \simeq 10$ s. The entire region between the equilibrium surface and the photosphere will be filled with optically thick plasma in a time of about $t_g \simeq 62$ min and will cause the observed strong depression in the spectrum. The expected density pulsations with a characteristic time of about t_g result in a corresponding variability of this feature, which could be detected by monitoring the depression with a time resolution of about t_g. A future discovery of such a variability of the UV depression band in the spectrum of GD 229 would constitute strong evidence in favour of our radiation-driven diskon model for this star. The radiation-driven envelope may be a source of X-rays similar to coronae of other stars. Unfortunately, the star has not been observed during ROSAT all-sky surveys. We suggest that future X-ray detections are to be attempted.

4. Conclusion

We have shown that cyclotron scattering in the atmosphere of a strongly magnetized white dwarf can support plasma against gravity on an equilibrium shell across closed field lines. Furthermore for a dipole field, matter can be supported in a disk like surface at the magnetic equator. However as the injection of plasma from the photosphere continues the increase of optical thickness inevitably leads to a collapse of the supported plasma onto the stellar surface and to a renewed cycle of plasma expulsion. We have determined the typical time scale of these pulsations. We have applied our results to the peculiar white dwarf GD 229. We propose that the observed UV depression results from cyclotron scattering of the extraordinary mode in the magnetosphere between the stellar surface and the equilibrium surface. We predict that the observed depression is variable on a time scale of the order of 1 hour.

Acknowledgements. This work is part of an ongoing cooperation between the Sterrekundig Instituut at Utrecht and the Institute of Applied Physics in Nizhny Novgorod and has been supported through NATO Laboratory Linkage Grant No. 921379. We like to thank the referee for valuable comments.

Appendix A

Since the dipole field decreases with distance from the star a photospheric cyclotron line, which is visible at a particular point in the magnetosphere does not overlap with the cyclotron resonance at this point if

$$\omega_B(1+3\sqrt{2}\beta_{T_\parallel}|\cos\alpha|) \le \min_{|\Theta_*-\Theta|\le \arccos 1/\rho} \{\omega_{B_*}(1-3\sqrt{2}\beta_{T_*}|\cos\alpha_*|)\}, \quad \text{(A1)}$$

where α is the angle between the magnetic field $\boldsymbol{B}$ in situ and a ray from this point to the origin of the photospheric cyclotron line, α_* is the angle between the same ray and the surface field $\boldsymbol{B}_*$ and Θ_* is the polar angle of this surface point with respect to the dipole axis. Since $\max\{\beta_{T_\parallel}, \beta_{T_*}\} \ll 1$, we can simplify the further analysis by putting $\alpha = \alpha_* = 0$. The border of the region (A1) can then be found with a perturbation technique. Inequality (A1) is valid for $\rho \ge \rho_{\rm line}(\Theta) + \Delta\rho_{\rm line}(\Theta)$, where $\rho_{\rm line}(\Theta) \gg \Delta\rho_{\rm line}(\Theta)$ and the function $\rho_{\rm line}(\Theta)$ is the solution of the unperturbed equation:

$$\sqrt{1+3\cos^2\Theta} = \rho^3 \min_{|\Theta_*-\Theta|\le \arccos 1/\rho} \{\sqrt{1+3\cos^2\Theta_*}\} \quad \text{(A2)}$$

Consider two possible cases. Firstly, if the magnetic equator is visible ($\Theta + \arccos(1/\rho) \ge \pi/2$), condition (A2) transforms into $\rho^3 = \sqrt{1+3\cos^2\Theta}$ which can only be satisfied for $\rho = 1$ and $\Theta = \pi/2$. Thus, $\rho_{\rm line}(\Theta = \pi/2) = 1$. Secondly, if the equator is not visible ($\Theta + \arccos(1/\rho) < \pi/2$), (A2) becomes

$$1+3\cos^2\Theta = \rho^6\left[1+3\left(\frac{|\cos\Theta|}{\rho} - \sin\Theta\sqrt{1-\rho^{-2}}\right)^2\right] \quad \text{(A3)}$$

This condition is met at $\rho_{\rm line}(\Theta) = \sqrt{x^2_{\rm line}(\Theta)+1}$, where $x_{\rm line}(\Theta)$ is determined by the equation $F(x,\Theta) = 1$ and

$$F(x,\Theta) = (x^2+1)^2\left(\frac{1+3\sin^2\Theta}{1+3\cos^2\Theta}x^2 - 2x\frac{3\sin\Theta|\cos\Theta|}{1+3\cos^2\Theta} + 1\right). \quad \text{(A4)}$$

Now perturbing (A3) in the following way:

$$F(x+\Delta x, \Theta) = \left[1+3\sqrt{2}(\beta_{T_\parallel}+\beta_{T_*})\right]^2, \quad \text{(A5)}$$

we get $\Delta\rho_{\rm line}(\Theta) \simeq x_{\rm line}\Delta x_{\rm line}/\rho_{\rm line}$, where

$$\Delta x_{\rm line}(\Theta) = 6\sqrt{2}(\beta_{T_\parallel}+\beta_{T_*})\left(\frac{\partial F}{\partial x}(x_{\rm line}(\Theta),\Theta)\right)^{-1}. \quad \text{(A6)}$$

Straightforward algebra then leads to (1).

References

Arons, J., 1987, in *IAU Symposium 125, The Origin and Evolution of Neutron Stars*, eds. D.K. Helfand, J.H.Huang, Reidel Publ. Cy., Dordrecht, p. 207

Bespalov, P.A., Serber, A.V., Zheleznyakov, V.V., 1990, in *Plasma Astrophysics, Proc. Joint Varenna-Abastumani-Nagoya-Potsdam-ESA Int. School and Workshop,* ed. T.D. Guyenne, ESA Publication Division, Noordwijk, p. 309

Bespalov, P.A., Zheleznyakov, V.V., 1990, Sov. Astron. Lett., 16, 442

Braun, A., and Yahel, R.Z., 1984, ApJ, 278, 349

Dahn, C.C., and 11 coauthors, 1982, AJ, 87, 419

Dermer C.D., Sturner S.J., 1991, ApJ, 382, L23

Forster, H., Strupat, W., Rösner, W., Wunner, G., Ruder, H., Herold, H., 1984, J. Phys. B, 17, 1301

Green R.F., Liebert J., 1981, PASP, 93, 105

Henry, R.J.W., O'Connel, R.F., 1985, PASP, 97, 333

Herold, H., Wolf K., Ruder, H., 1987, Astrophys. Space Sci., 131, 591

Lucy, L.B., Solomon, P.M., 1970, ApJ, 159, 879

Mitrofanov, I.G., 1986, Sov. Astron., 30, 57

Mitrofanov, I.G., Pavlov, G.G., 1982, MNRAS, 200, 1033

Schmidt, G.D., Latter, W.B., Foltz, C.B., 1990, ApJ, 350, 758

Sturner S.J., Dermer C.D., 1992, in *Gamma- Ray Bursts. AIP Conference Proceedings 265,* eds. W.S.Paciesas and G.J.Fishman, AIP, New York, 277

Sturner, S.J., and Dermer, C.D., 1994, Astron. Astrophys., 284, 161

West, S.C., 1989, ApJ, 345, 511
Zheleznyakov, V.V., 1981, Astrophys. Space Sci., 77, 279
Zheleznyakov, V.V., 1984, Sov. Sci. Rev. E Astrophys. Space Phys., 3, 157
Zheleznyakov, V.V., Litvinchuk, A.A., 1984, Astrophys. Space Sci., 105, 73
Zheleznyakov, V.V., Litvinchuk, A.A., 1986, in *Plasma Astrophysics, Proc. Joint Varenna-Abastumani Int. School and Workshop,* eds. T.D.Guyenne and L.M.Zeleny, ESA Publication Division, Noordwijk, p. 375
Zheleznyakov, V.V., Litvinchuk, A.A., 1987, Sov. Astron., 31, 159
Zheleznyakov, V.V., Serber, A.V., 1991, Sov. Astron. Lett., 17, 179
Zheleznyakov, V.V., Serber, A.V., 1994, ApJ Suppl., 90, 783.

This article was processed by the author using Springer-Verlag LaTeX A&A style file version 3.